Electrostatic Fluid Structure Interaction (EFSI) on the Huygens Experiment

R. Godard[*,1], J. de Boer[2], N. Ibrahim[3], G. Molina-Cuberos[4]
1 Depart. of Mathematics and Computer Science, Royal Military College of Canada
2 Physics Department, Royal Military College of Canada
3 Institute for Aerospace Studies, University of Toronto, Canada
4 Depto. Fisica, Facultad de Quimica, Campus Espinardo, Murcia, Spain
*R. Godard: Depart. of Mathematics and Computer Science, Royal Military College of Canada, Kingston (On.) K7K 7B4, Canada, godard-r@rmc.ca

Abstract: The Huygens Atmospheric Structure Instrument (HASI) was designed to characterize the physical properties of the lower atmosphere and the surface of Titan, the planet-size moon of Saturn. The Relaxation Probe (RP) sensor on the Huygens probe, determined the electrical conductivity in the lower atmosphere of Titan, from 140 km to ground. An hypothesis was that at an altitude above 100km, the booms were not fully deployed, and a contamination of measurements could occur. In this present work, we numerically study this geometrical effect, which is linked to the electrostatic fluid structure interaction (EFSI) between the vessel and the RP. The mathematical model of the electrostatic interaction between the vessel and the RP consists in solving linear elliptic partial differential equations with finite element methods, for a complex geometry, with boundary conditions for the electric potential and the electron number density. We were able to obtain lower and upper bounds for the interaction. We suggest that for future experiments, the boom should act as a biased guard ring, and that the RP electrode to be positioned at a distance of 50cm from the surface of the vessel.

Keywords: Titan atmosphere, Relaxation Probe, electron conductivity, Fluid Structure Interaction.

1.Introduction

The Huygens probe entered and successfully descended into Titan's atmosphere on January 14th, 2005. This experiment has already been the subject of many scientific publications (Béghin et al., 2007; Grard et al., 2006; Hamelin et al., 2007; Lopez-Moreno al, 2008; Molina-Cuberos et al. 2010). This present work differs from the previous ones, because it deals with some technical questions which were not considered in the previous publications. Briefly, the Huygens Atmospheric Structure Instrument (HASI) was designed to characterize the physical properties of the lower atmosphere and surface of Titan, the planet-size moon of Saturn. The electrostatic Relaxation Probe (RP) sensor on the Huygens probe was designed to determine the electrical conductivity in the atmosphere of Titan, from around 140 km to the ground. Comparative results obtained from the Mutual Impedance Probe (MIP), an independent instrument for air conductivity measurements, implied that, in the RP data processing for the electron conductivity, a geometrical factor D_λ related to the ratio of radius a_{RP} of the electrode to the electron Debye length, must be included. The Debye length is defined as $\lambda_D = \sqrt{\frac{\varepsilon_0 k_B T}{N_e e^2}}$, where ε_0 is the permittivity in vacuum, k_B is the Boltzmann constant, T is the temperature, N_e the electron number density, and e is the elementary charge. From a very careful analysis, we were able to reduce the initial discrepancies between MIP and RP results from a factor 10 to 20 to a factor 2. Even if now RP results compare very positively with a completely independent method, the MIP, in this present work, we would like to track other possible sources of errors such as the interaction between the vessel and RP. We call this later effect, the Electrostatic Fluid Structure Interaction (EFSI). Here, EFSI is divided into two sections: a) the effect of the distance between the RP and the vessel, and the influence of the potential of the vessel on the RP electron current collection, and b) if the ratio of the "size" of geometries between RP and vessel is not adequate, the vessel reference potential is not stable and may contaminate RP signals. In

section 4, we shall specify the "size" of geometries.

Firstly, let us present some geometrical, electrical and mechanical properties of the system RP-vessel. Figure 1 represents the parachute, the vessel and the sensors. The electrical conductivity sensors were placed on two deployable booms, and consist of two conducting disks (RP1, RP2) forming a double relaxation probe and four ring electrodes (RX1,TX1, RX2, TX2) forming the MIP.

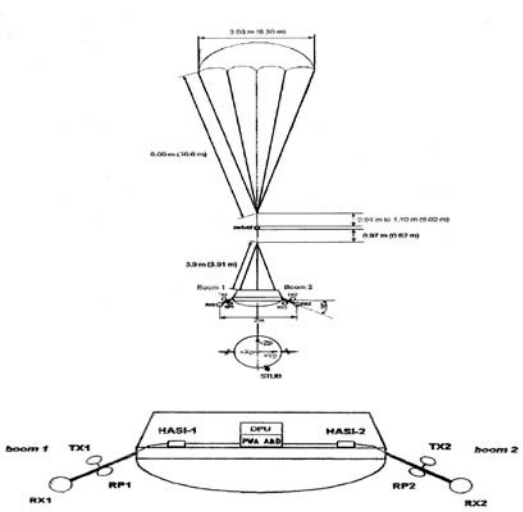

Figure 1: the Huygens experiment with the parachute, the vessel and the sensors.

The RP experimental set-up consists of an electrode that is biased at a negative or positive potential with respect to a reference level, which is linked to the vessel potential. Here, we shall only consider the electron collection at positive potentials. Figure 2 represents a schematic view of the RP, where the output signal is the relaxation response to an input potential Dirac distribution:

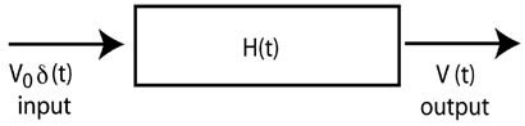

Figure 2: The electronic schema of the RP sensor

This relaxation signal corresponds to the discharge of an equivalent R_eC_e circuit, where R_e and C_e are respectively the resistance and the capacitance of the system formed by the electrode and the ionized medium. In a simplified theory for the Relaxation Probe, the electron conductivity σ_e is given by:

$$\frac{\sigma_e}{\varepsilon_0} = \frac{1}{R_eC_e} \quad (1)$$

In order to reduce the speed of decay of the electrode potential for a given conductivity, a shunt capacitor C_*=352.5 pF was connected in parallel to this RP2 sensor. For the Huygens experiment, the RP electrode is a circular disk of radius a_{RP} = 3.5 cm. The sensor is mounted on a boom at a distance of 15 cm from the vessel. For modeling purposes, we shall assume that the vessel is equivalent to a sphere of 0.6 m radius. By conformal mapping, we can simulate the RP sensor by a small sphere of radius of 2.28 cm.

Secondly, we would like to present the environmental conditions of the experiment, and the properties of the neutral flow around the vessel. Figure 3 shows the Huygens velocity profile as a function of altitude.

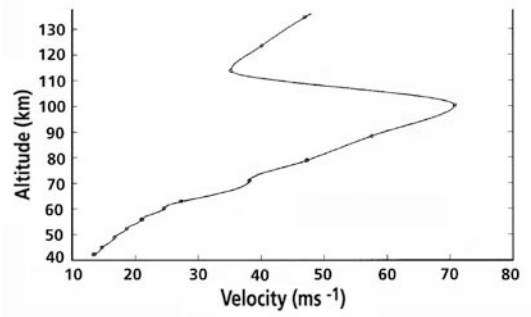

Figure 3: Velocity variation with altitude during Huygens probe descent

Around the altitude of 110 km, the velocity increased drastically from 40 m/s before the second parachute release up to 70 m/s. Then, the velocity decreased gradually and smoothly. Hamelin (2007) emphasized that at altitudes above 100 km, only an incomplete boom opening could give MIP impedance values matching the data. Then for RP there were roughly three possibilities: a) active boom opened given good RP signals, b) active boom partially opened giving biased RP data, and, c) both booms partially deployed giving again biased RP data. Our objective was to try to estimate these bias.

2. The Computational Fluid Dynamics

A Computational Fluid Dynamics (CFD) analysis was carried out at the University of Toronto (Ibrahim, 2009) in order to determine the variation of the neutral density and flow pattern in the neighbourhood of the Huygens

probe at altitudes of 130 km, 100 km and 50 km. Explicit and implicit (Newton-Krylov-Schwarz) methods were used to resolve both inviscid and turbulent flows. For this 2D flow, the vessel was designed using a variety of predefined piecewise splines. Once the solution space is defined, it is meshed using a flexible block-based hierarchical data structure to be used for the finite-volume method. Now, we would like to briefly describe the flow conditions at the altitude of 100 km. The temperature T was $145^o K$, the pressure was 0.954 kPa, the Mach number was around 0.1445. The Reynolds number is plotted on Figure 4. It did vary from 10^7 to 2.6×10^7 with a peak around 60 km of altitude. It is apparent that the flow during the descent was turbulent.

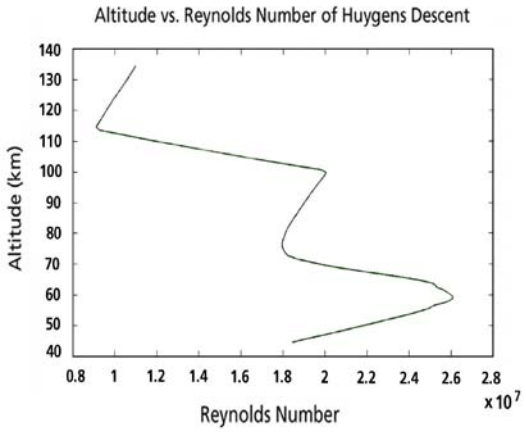

Figure 4: Reynolds number variation with altitude

Due to the limited space, our results will be presented only for the 100 km altitude.
Figure 5 represents the neutral density distribution for Huygens at this altitude.

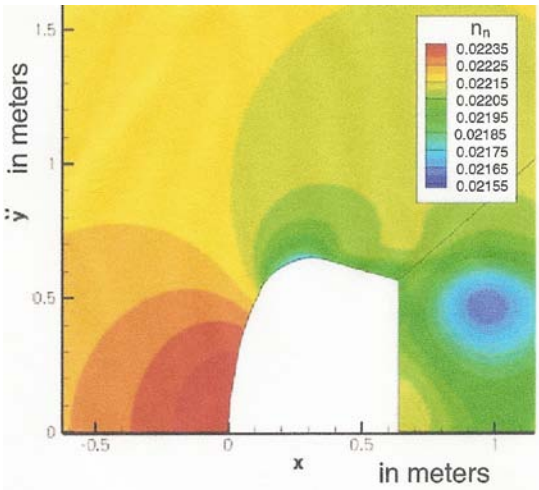

Figure 5: Density distribution for Huygens

From the CFD analysis, we observed that the density distribution was almost identical to its ambient value at the vessel surface, and also at the MIP and RP locations. Because the neutral density is linked to the electron conductivity and the electron number density, it was important to know that the neutral density was almost a constant at a given altitude, and had no important flow effect. Another challenging CFD problem came from the analysis of low frequency electromagnetic waves (ELF) detected my MIP (Béghin, 2007). We quote Beghin: "Since there is an apparent correlation between the exchange of parachutes and a sudden enhancement of the 36 Hz line and ELF broadband noise, any artifact related to this event must be investigated seriously." However airframe noise is difficult to simulate numerically.

3. The interaction vessel-RP: EFSI

3.1 Governing equations and computational domain

If the boom is not fully deployed at altitudes above 100km, can we consider the hypothesis of a shadowing effect of the vessel on the RP sensor? For example, this shadowing effect may affect the RP current collection, the resistance R_e and capacity C_e. In order to simplify the computational model, we shall consider an axisymmetrical problem, and therefore, we shall make the following assumptions: the vessel is simulated by a sphere of an equivalent radius 0.6 m, and the RP sensor is approximated by a small sphere of radius 0.0228 m. We neglect the boom effect, the vicinity of another RP sensor, and MIP electrodes. In the Huygens experiment, the boom was an insulator, but it introduced numerical instabilities in the simulation process. We assumed that the RP has no effect on the vessel potential, that we consider, for simplicity's sake, to be zero. The RP current collection described by a fluid mathematical model for electrons, positive ions and negative ions, but negative ions have a negligible contribution. Indeed the vessel and RP introduce potential perturbations which are described by a Poisson equation for a 2D problem with a cylindrical symmetry. We call our problem an Electrostatic Fluid Structure Interaction (EFSI). Neglecting fluid dynamics effects, the governing conservative equation for the electron number

density is the following elliptic partial differential equation (Swift and Schwar, 1969):

$$-\nabla^2 n_e + \nabla n_e . \nabla \varphi + n_e \nabla^2 \varphi = 0 \qquad (2)$$

where $n_e = \frac{N_e}{N_{e,\infty}}$ is the non-dimensional electron number density, $N_{e,\infty}$ is the ambient value far from the system between the sensor and the vessel, $\varphi = \frac{eV}{k_B T}$ is the non-dimensional potential and *V* is the electric potential in the computational domain. The density equations are linked together to a non-dimensional Poisson equation for the electric potential as follows:

$$\nabla^2 \varphi = -D_\lambda^2 (n_i - n_e) \qquad (3)$$

Where D_λ is the Debye ratio we introduced at the beginning of our paper, and n_i is the non-dimensional ion number density. In the Huygens experiment, we have $0.07 \le D_\lambda \le 1.50$ for RP (Molina-Cuberos, 2010). As a first approximation, we shall assume $D_\lambda = 0$, i.e., we approximate a Poisson equation by a Laplace equation. And the model becomes linear. From our experiment electron density profile, it was a highly acceptable approximation above 100 km of altitude. Given the boundary conditions for the electric potential, the Laplace electric potential is the input to the electron density equation. Figure 6 describes our finite element computational domain with the boundary conditions for the electric potential and the electron number density.

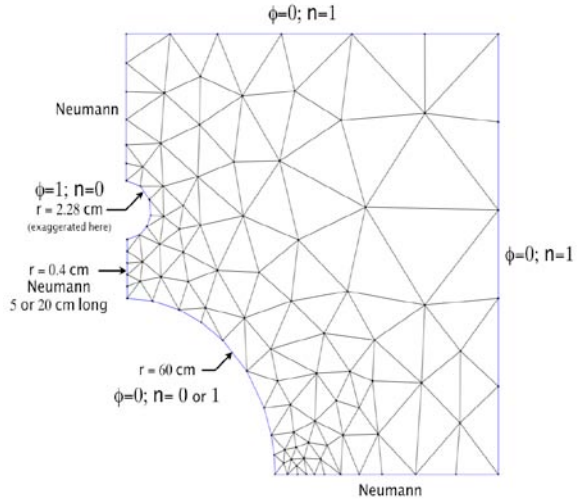

Figure 6: The EFSI computational domain

From the axial symmetry, we represent only a quarter of the vessel and half of the RP. This could be done by COMSOL. Out the outer boundaries of the computational domain, the electric potential is set to zero except at the RP surface, where it is the applied potential φ_{RP} and in the regions where Neumann conditions apply. We already said that the simulation of the boom introduced strong electric fields at the vicinity of the RP, and made our system to diverge. Of course, these strong electric fields are real, and the only way to overcome them is to replace the insulator by a biased guard ring. However, this will be equivalent to an addition to the RP electron current which may have the unwanted effect to drift the vessel potential (section 4). The density boundary conditions are more complex. At the outer boundaries, the density has its ambient value. When the Neumann condition applies for the electric potential, it applied too for the electron number density. Our main concerns are the electron number density surface conditions for RP and the vessel.

From the electrostatic probe theory in a continuum plasma, the RP surface boundary condition would be (Swift and Schwar, 1969):

$$n_{RP} = \frac{1}{1 + Xa_{RP}} \qquad (4)$$

Where X is a complex equation. In the limit $Xa_{RP} \to +\infty$, $n_{RP} = n_V = 0$. This corresponds to the classical diffusion (pressure) boundary conditions. On the other hand, Ibrahim's work (2009) on the CFD around the Huygens vessel (Figure 5) indicated that for the neutral flow, the neutral density at the vessel surface is $n_{n,V} = 1$. Fluid Dynamics (FD) effects may modify the surface boundary conditions.

Firstly, let us consider a 1D Laplace model for RP, i.e., we consider that RP is far enough from the vessel that there is no shadowing effect, say that the distance *d* from the surface of RP to the vessel is 30 cm to 50 cm. Assume that the surface boundary condition is $n_{e,RP} = \alpha$, with α a percentage, $0 \le \alpha \le 1$. We proved that the collected current is roughly insensitive to the

value α, as long as the RP potential is large enough. However, if we replace the Laplace equation by a Poisson equation, the condition $n_{e,RP}=1$ is impossible. In this case, and simplicity's sake, assume a power-law potential profile of the type $\varphi(r)=\varphi_{RP}\left(\frac{a_{RP}}{r}\right)^n ; n>1$, then the attracted collected current would be enhanced with respect to the Laplace approximation. This would be a violation of what it is observed theoretically and experimentally. For the Huygens experiment, we selected the classical diffusion (pressure) boundary condition $n_{e,RP}=0$ (Molina-Cuberos, 2010). Once the RP density surface condition was fixed, the problem was to select a density surface boundary condition for the vessel. For the vessel, we assume no electric potential effect $\varphi_V=0.$ Which effect was dominant: the fluid dynamics condition with $n_{e,V}=1$ or the diffusion condition $n_{e,V}=0$? For electrons, it is not the Reynolds number (Figure 4) which is important, but the electron diffusion Reynolds number $R_d=\frac{2Ua_V}{D_e}$ where U is the flow velocity, and D_e is the electron diffusion coefficient. We found low values: $17\le R_d\le 337$. Indeed we could have also computed the ratio between the diffusion current and the fluid dynamics (FD) current. They were comparable for the first 3 measures, then the FD current dominated. Don't forget that for a collisionless regime, the electron number density is one-half of its ambient value for $\varphi_V=0$. This is due to a shadowing effect of the object where particles can't reach the surface from inside the body. Therefore, we decided to make two runs for the two boundary vessel surface conditions. Results are discussed in the following section.

3.2 Results and discussion: applications to data processing of RP sensors

Firstly, the numerical stability of our scheme was verified by trial and errors for various distances *d*. The main purpose of the simulation was to try to discuss various possibilities for the upper part of the flight, where the problem of boom opening could occur. For a potential $\varphi_{RP}=500$, we selected two distances $d=5$ cm and *d* = 20 cm, and two vessel boundary conditions. Results are presented on table 1. We see that capacities are fairly insensitive to vessel boundary conditions. We obtained a 12% difference. If the vessel boundary condition is set to $n_{e,RP}=1$, the normalized to unity time constant RC is not affected. However, for $n_{e,RP}=0$, we found an increase by a factor 7 for *d* = 5 cm, and almost a factor 3 for *d = 20* cm.

phi_RP=500

units:	Capacitance epsilon_0 * 1 m	Vessel B.C.	Resistance phi_RP/Flux	RC
5 cm boom	0,3363	n_v=1	2,99	1,01
		n_v=0	21,97	7,39
20 cm boom	0,3002	n_v=1	3,34	1,00
		n_v=0	9,75	2,93

Table 1: Results of the numerical simulation of the system RP-vessel and the equivalent normalized RC network for two vessel boundary conditions

From these results, we found a lower bound and an upper bound for the EFSI. Even it is just a hypothesis, a factor 3 (an over-estimation) of our errors could well explain the discrepancies between RP and MIP results. A factor 3 would mean that the apparent RP conductivity was too low. It is an upper bound because an exact simulation should be done, not for a Laplace approximation by through a Poisson equation (Eq. 3). In this case, potential decays are steeper, and less sensitive to the vessel boundary conditions (Godard, 2007). The factor 7 would mean that the apparent conductivity measurements should be taken with caution for the three measures above 100km. Again this is just a hypothesis. As a problem of optimal design, we suggest for future planetary missions what RP would be located at 40 to 50 cm from the vessel.

The next figures represent the normalized electron number density n_e map and for two values of the distance *d*. We observe some kind of numerical noise between RP and the vessel.

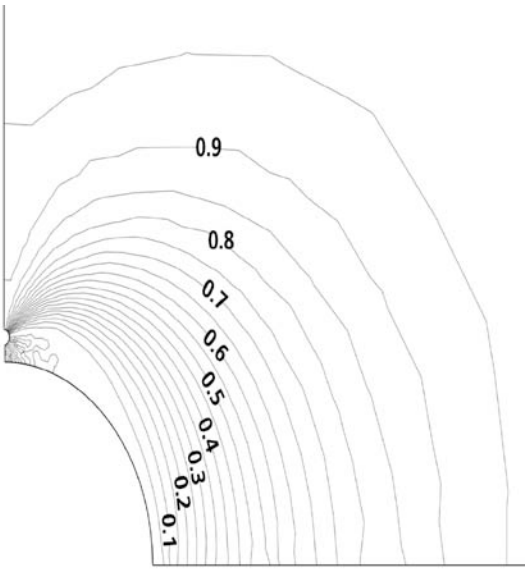

Figure 7: electron density map around the system vessel-RP, for a distance d = 5 cm, and a vessel boundary condition $n_{e,V} = 0$.

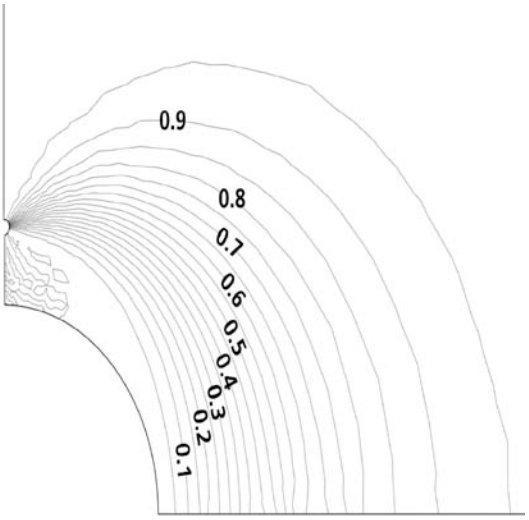

Figure 8: electron density map around the system vessel-RP, for a distance d = 20 cm, and a vessel boundary condition $n_{e,V} = 0$.

3.3 Applications to data processing

In the hypothesis that the vessel-RP interaction does exist, we should take it into account for RP data processing. For the Huygens experiment we developed a more complex data processing scheme where parameters of a mathematical model, i.e. mainly the electron conductivity are adjusted through a minimum deviation algorithm. It would become a three-variable minimisation process if we take into account the shadowing effect of the vessel.

4. The vessel potential

In this mathematical model, we assume that the system RP-vessel acts as an asymmetric double probe. This hypothesis is also used in terrestrial ionospheric or magnetospheric studies where the spacecraft potential is the reference potential. Under this hypothesis and for the Huygens experiment and equivalent electronic network will act as follows (Figure 9).

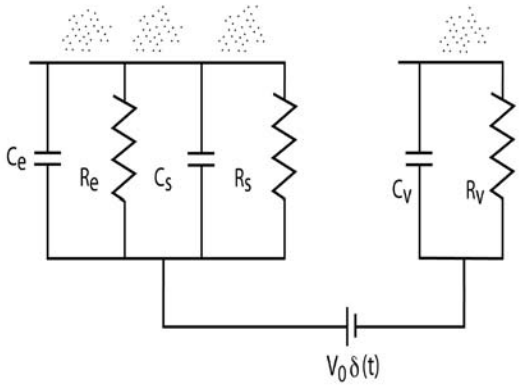

Figure 9: the equivalent electronic network for the system RP-vessel

Let us consider that the system vessel-medium has its own resistance R_V and capacity C_V, while, for the RP electrode, we have additional shunt resistance C_s and capacity C_s to the circuit $R_e C_e$. With this model, the constraint comes from the total collected current, which must be equal to zero. When the RP is strongly positively biased, the vessel must compensate this current. Now, with our circuit, the RP electron current has opposite sign to the one collected by the vessel. Without doing complex simulations of the double probe system, let us comment on the contribution of all collected currents. Firstly, because of its low conductivity, the positive ion current is small in comparison to the electron current, also the fluid dynamics current or the natural electric field contribution are constant. The only possibility is that the RP electrode is strongly positively biased, the vessel potential must drift in the same direction, i.e., towards positive potentials so that the attracted electron vessel current does increase. As a

result, the RP potential must drift towards lower potentials, so that the current conservation is not violated. As a first approach, and neglecting all other sources of current, let us assume that the electron RP current is directly compensated by the attracted electron vessel current:

$$4\pi a_{RP}\sigma_e k_B T / q_e (1+\varphi_{RP}{}^{\beta_e}) = 4\pi a_V \sigma_e k_B T / q_e (1+\varphi_V{}^{\beta_V}) \quad (5)$$

Where a_V is the equivalent vessel radius, and exponents β_e and β_V come from a parameter fit for the current (Molina-Cuberos, 2010) as a function of potential φ and parameter D_λ which was defined in the introduction. As a first order approximation, let us consider $\beta_e = \beta_V = 1$, i.e. to a Laplace distribution of potential in the vicinity of the system RP electrode-vessel. Under these conditions, we observe that the vessel potential does not depend upon the electron conductivity, but only on the ratio of radii:

$$\varphi_V \simeq \frac{a_{RP}}{a_V}\varphi_{RP} \quad (6)$$

With $a_V = 0.6$ m, $a_{RP} = 0.0228$ m, we obtain a 4% ratio, i.e. if $\varphi_{RP} = 1000$, then $\varphi_V = 40$. If the Laplace approximation is not fulfilled, the vessel potential will drift by a substantial amount. This situation may occur during plateaus, or if during terrestrial flights, the vessel encounters very strong natural electric fields or FD effects which can perturb the vessel potential and its stability. Indeed this situation can only occur for large attracting electrode potentials. It is interesting to make a comparison with ionospheric experiments where the stability of the measurements for electrostatic probes depends upon the return area of the spacecraft and not the size of the geometry.

5. References

Béghin C. et al., A Schuman-like resonance on Titan driven by Saturn's magnetosphere possibly revealed by the Huygens Probe, *ICARUS*, **191**, pp. 251-266 (2007)

Godard R., Sheath and potential profiles around RP sensors and the gondola on the Huygens experiment, Proceedings of the COMSOL conference , pp. 225-232, (2007)

Grard, R., et al., Electric properties and related physical characteristics of the atmosphere and surface of Titan, *Planet. Space Sci.*, **Vol. 54**, pp. 1124-11362 (006)

Hamelin, M., et al., Electron conductivity and density profiles derived from the mutual impedance probe measurements performed during the descent of Huygens through the atmosphere of Titan, *Planet. Space* Sci., **Vol. 55**, pp.1964-1977 (2007)

Ibrahim, N., CDF Analysis of Huygens probe in Titan's Atmosphere. Unpublished 4Th year thesis, University of Toronto, Institute for Aerospace Studies, Toronto (2009)

Lopez-Moreno, J.J. et al., Structure of Titan's low altitude ionized layer from the Relaxation Probe onboard HUYGENS, *Geophys. Res. Lett.*, **35**, L22104 (2008)

Molina-Cuberos, G.J. et al., A new approach in estimating Titan's electron conductivity based on data from Relaxation Probe sensors on the Huygens Experiment, submitted to *Planet. Space Sci.* (2010)

Swift, J.D. and Schwar, M.J.R., *Electric Probes for Plasma Diagnostics*. London Iliffe Books, London (1969)

6. Acknowledgements

One of the authors (R.G.) would like to acknowledge the whole Huygens scientific team for their interest in this work, and more particularly C. Béghin, R. Grard, M. Hamelin and J.J. Berthelier and C. Groth for exchange of ideas and invaluable discussions and suggestions.